



Phyllanthus tenellus Roxb. and *Kaempferia parviflora* Wall. ex Baker compounds as inhibitors of SARS-CoV-2 main protease and RNA-dependent RNA polymerase: A molecular docking study

[Compuestos de *Phyllanthus tenellus* Roxb. y *Kaempferia parviflora* Wall. ex Baker como inhibidores de la proteasa principal del SARS-CoV-2 y de la ARN polimerasa dependiente de ARN: Un estudio de acoplamiento molecular]

Suhaina Supian*, Muhamad Aizzuddin Ahmad, Lina Rozano, Machap Chandradevan, Zuraida Ab Rahman

Biotechnology and Nanotechnology Research Centre, Malaysian Agricultural Research and Development Institute (MARDI), Serdang 43400, Selangor, Malaysia.

*E-mail: suhaina@mardi.gov.my

Abstract

Context: The outbreak of a novel coronavirus, SARS-CoV-2 has caused an unprecedented COVID-19 pandemic. To put an end to this pandemic, effective antivirals should be identified or developed for COVID-19 treatment. However, specific and effective antivirals or inhibitors against SARS-CoV-2 are still lacking.

Aims: To evaluate bioactive compounds from *Phyllanthus tenellus* and *Kaempferia parviflora* as inhibitors against two essential SARS-CoV-2 proteins, main protease (M^{pro}) and RNA-dependent RNA polymerase (RdRp), through molecular docking studies and to predict the drug-likeness properties of the compounds.

Methods: The inhibition potential and interaction of *P. tenellus* and *K. parviflora* compounds against M^{pro} and RdRp were assessed through molecular docking. The drug-likeness properties of the compounds were predicted using SwissADME and AdmetSAR tools.

Results: Rutin and ellagic acid glucoside from *P. tenellus* and 4-hydroxy-6-methoxyflavone and 5-hydroxy-3,7,4'-trimethoxyflavone from *K. parviflora* exhibited the highest binding conformations to M^{pro} by interacting with its substrate binding site that was predicted to halt the M^{pro} activity. As for RdRp, ellagitannin and rutin from *P. tenellus* and peonidin and 5,3'-dihydroxy-3,7,4'-trimethoxyflavone from *K. parviflora* were the best-docked compounds that bound to the RdRp catalytic domain (Asp760 and Asp761) and NTP-entry channel that were anticipated to stop RNA polymerization. However, in the context of drug developability, 4-hydroxy-6-methoxyflavone, 5-hydroxy-3,7,4'-trimethoxyflavone, peonidin and 5,3'-dihydroxy-3,7,4'-trimethoxyflavone from *K. parviflora* were highly potential to be oral active drugs compared to rutin, ellagic acid glucoside and ellagitannin from *P. tenellus*.

Conclusions: *P. tenellus* and *K. parviflora* compounds, particularly the aforementioned compounds, were suggested as potential inhibitors of SARS-CoV-2 M^{pro} and RdRp.

Keywords: antiviral; compounds; COVID-19; *in silico*; *Kaempferia parviflora*; *Phyllanthus tenellus*.

Resumen

Contexto: El brote de un nuevo coronavirus, el SARS-CoV-2, ha provocado una pandemia de COVID-19 sin precedentes. Para poner fin a esta pandemia, es necesario identificar o desarrollar antivirales eficaces para el tratamiento del COVID-19. Sin embargo, aún se carece de antivirales o inhibidores específicos y eficaces contra el SARS-CoV-2.

Objetivos: Evaluar compuestos bioactivos de *Phyllanthus tenellus* y *Kaempferia parviflora* como inhibidores contra dos proteínas esenciales del SARS-CoV-2, la proteasa principal (M^{pro}) y la ARN polimerasa dependiente del ARN (RdRp), mediante estudios de acoplamiento molecular y predecir las propiedades de similitud con los fármacos de los compuestos.

Métodos: El potencial de inhibición y la interacción de los compuestos de *P. tenellus* y *K. parviflora* contra la M^{pro} y la RdRp fueron evaluados mediante docking molecular. Las propiedades de semejanza de los compuestos se predijeron mediante las herramientas SwissADME y AdmetSAR.

Resultados: La rutina y el glucósido del ácido elágico de *P. tenellus* y la 4-hidroxi-6-metoxiflavona y la 5-hidroxi-3,7,4'-trimetoxiflavona de *K. parviflora* mostraron las conformaciones de unión más altas a M^{pro} al interactuar con su sitio de unión al sustrato que se predijo para detener la actividad de M^{pro}. En cuanto a la RdRp, la elagitanina y la rutina de *P. tenellus* y la peonidina y la 5,3'-dihidroxi-3,7,4'-trimetoxiflavona de *K. parviflora* fueron los compuestos mejor acoplados que se unieron al dominio catalítico de la RdRp (Asp760 y Asp761) y al canal de entrada NTP que se anticipó que detendría la polimerización del ARN. Sin embargo, en el contexto del desarrollo de fármacos, la 4-hidroxi-6-metoxiflavona, la 5-hidroxi-3,7,4'-trimetoxiflavona, la peonidina y la 5,3'-dihidroxi-3,7,4'-trimetoxiflavona de *K. parviflora* tendrían un gran potencial para ser fármacos activos por vía oral en comparación con la rutina, el glucósido de ácido elágico y la elagitanina de *P. tenellus*.

Conclusiones: Los compuestos de *P. tenellus* y *K. parviflora*, en particular los mencionados, fueron sugeridos como potenciales inhibidores de M^{pro} y RdRp del SARS-CoV-2.

Palabras Clave: antiviral; compuestos; COVID-19; *in silico*; *Kaempferia parviflora*; *Phyllanthus tenellus*.

ARTICLE INFO

Received: August 19, 2022.

Accepted: November 2, 2022.

Available Online: November 22, 2022.

AUTHOR INFO

ORCID: 0000-0003-0938-7443 (SS)

0000-0002-6182-2089 (LR)

0000-0002-3249-2690 (ZAR)

Abbreviations: ADMET: Absorption, distribution, metabolism, excretion, and toxicity; BBB: Blood-brain barrier; COVID-19: Coronavirus disease; GI: Gastrointestinal; M^{pro}: Main protease; P-gp: P-glycoprotein; RdRp: RNA-dependent RNA polymerase; RMSD: root mean square deviation; SARS-CoV-2: Severe acute respiratory syndrome coronavirus 2.

INTRODUCTION

COVID-19, an unprecedented pandemic of acute respiratory infection that emerged in late 2019, is caused by the *Coronaviridae* family member, severe acute respiratory syndrome coronavirus-2 (SARS-CoV-2). SARS-CoV-2, which belongs to the same genus of betacoronaviruses such as SARS-CoV and MERS-CoV, shares 79% of its genome sequence with SARS-CoV and 50% with MERS-CoV (Zhu et al., 2020). The SARS-CoV-2 genome comprises approximately 30 Kb positive sense RNA encoding structural and non-structural proteins (nsps). Structural proteins such as spike, nucleocapsid, envelope, and membrane proteins are prominently involved in viral assembly (Tai et al., 2020). On the other hand, nsps are required for viral RNA transcription and genome replication (Zhou et al., 2020). These nsps are produced from the cleavage of the viral polyproteins Pp1a and Pp1ab by two cysteine proteases, main protease (M^{pro}) and papain-like protease, resulting in 16 different proteins (nsp1-nsp16) with numerous functions. Thus, the cleavage process is crucial as it involves the release of essential proteins such as RNA-dependent RNA polymerase (nsp12) and helicase (nsp13), which are critical for the viral life cycle.

Due to the importance of M^{pro} and RdRp roles, these proteins have been the main targets for the discovery of therapeutic agents against SARS-CoV-2. These proteins are also highly conserved among the other coronaviruses and between SARS-CoV-2 variants (Vangeel et al., 2022). Thus, the inhibitors or drugs targeting M^{pro} and RdRp should have a broad-spectrum antiviral activity, and they will remain effective against future emerging variants (Goyal and Goyal, 2020). The recent availability of M^{pro} and RdRp information and structures has aided in the drug discovery process for these proteins. Jin et al. (2020) have first identified the crystal structures of SARS-CoV-2 M^{pro} in complex with peptide inhibitor N3 (PDB ID: 6LU7). The SARS-CoV-2 RdRp cryo-electron microscopy structure in complex with cofactors, nsp7 and nsp8 (PDB ID: 6M71) has also been recently discovered (Gao et al., 2020). Many scientists all over the world have benefited from this information in strategizing the identification or development of drugs or antivirals against SARS-CoV-2 (Ghanimi et al., 2022; Kharisma et al., 2022). The idea of utilizing repurposing drugs such as remdesivir, nelfinavir, and nirmatrelvir has been proposed and tested to be effective in COVID-19 clinical trials, but they exhibited adverse effects, including blood clots, gastrointestinal upset,

respiratory failure, and organ dysfunction (Lamb, 2022; Mohammad Zadeh et al., 2021). Therefore, safe and effective antivirals against SARS-CoV-2 are still highly needed.

Plants have been receiving major attention in the development of antivirals by the pharmaceutical industry as they contain many different bioactive molecules with numerous therapeutic properties. Plant bioactive compounds were safer and more effective than synthetic drugs (Babar et al., 2013). Moreover, plant extracts and their isolated compounds have been proven to have antiviral activities against various viral diseases (Ben-Shabat et al., 2020). Saikosaponins, a plant compound found in Chinese herb, *Bupleurum* spp., for instance, have an antiviral effect against human coronavirus 229E (Cheng et al., 2006). The aqueous extract of *Prunella vulgaris* also exhibited antiviral activity against HIV by interfering with the virion post-binding events (Oh et al., 2011). Hence, the exploration and screening of plants with antiviral effects is a promising approach for the search of antivirals.

Phyllanthus tenellus Roxb. (family *Phyllanthaceae*) and *Kaempferia parviflora* Wall. ex Baker (family *Zingiberaceae*) are two prevalent herbs with numerous therapeutic properties. *P. tenellus* was found to be able to treat hepatitis B, inflammatory bowel disease, diabetes, and urolithiasis (Silva et al., 2012). In addition, this herb contains a high level of hydrolyzable tannins, which are known to be associated with antiviral activity (Mohd Jusoh et al., 2019; Tan et al., 2013). Likewise, *K. parviflora*, locally known as black ginger, was also proven to have medicinal benefits for various diseases (Chen et al., 2018). Methoxyflavone, the main compound in *K. parviflora*, inhibited HIV-1 protease activity (Sookkongwaree et al., 2006). Moreover, *K. parviflora* extracts significantly suppressed the replication of the highly pathogenic avian H5N1 influenza virus (Sornpet et al., 2017). However, the antiviral properties of *P. tenellus* and *K. parviflora* against SARS-CoV-2 have never been evaluated and discussed.

Hence, in the present study, we screened the bioactive compounds from *P. tenellus* and *K. parviflora* with inhibition potential against SARS-CoV-2 M^{pro} and RdRp through molecular docking. The interactions of the compounds with M^{pro} and RdRp were elucidated. In addition, *in silico* drug-likeness and ADMET analysis were also performed to predict the compound's suitability as an active oral drug. This study is crucial in providing a promising solution for the treatment of COVID-19.

MATERIAL AND METHODS

Ligands preparation

The information on the 19 bioactive compounds from *P. tenellus* was obtained from Mohd Jusoh et al. (2019), and the 20 compounds from *K. parviflora* was obtained from Yenjai et al. (2004) and Chen et al. (2018). The compound structures were retrieved from the PubChem database (<https://pubchem.ncbi.nlm.nih.gov/>). The repurposing drugs, nelfinavir and hydroxychloroquine were used as controls for M^{pro}, whereas remdesivir and hydroxychloroquine were controls for RdRp. All the compounds were energy-minimized and converted into pdbqt format using Open Babel version 2.3.

Receptor preparation

The crystal structures of COVID-19 M^{pro} in complex with an inhibitor N3 (PDB ID: 6LU7) and the cryo-electron microscopy structure of RdRp in complex with nsp7 and nsp8 (PDB ID: 6M71) at 2.16 Å and 2.9 Å, respectively, were retrieved from Protein Data Bank (PDB) (<http://www.rcsb.org>). Water molecules, hetero atoms, and inhibitors were removed, whereas hydrogen atoms were added to the protein structure using Discovery Studio Visualizer v19.1.0.18287 (BIOVIA, San Diego, CA, USA).

Molecular docking

The grid box was set at the catalytic site of M^{pro} with a size of 40 × 40 × 40 points and centered at coordinates of x = -11.053, y = 15.622, and z = 67.602. As for RdRp, the grid box covering the active site was set at a size of 30 × 30 × 30 points and coordinates of 114.52, 114.11, and 122.91. The tolerance of root means square deviation (RMSD) was set to 2.0 Å. The docking simulation was carried out using Autodock Vina version 1.1.2. The docked complexes with the lowest binding energy (kcal/mol) were selected, and their hydrogen and/or hydrophobic interactions were visualized using PyMOL version 2.4.0 (Schrodinger, LLC) and BIOVIA Discovery Studio Visualizer v19.1.0.18287 (BIOVIA, San Diego, CA, USA).

The docking procedure was validated by redocking the co-crystallized native ligand N3 inhibitor on M^{pro} using the same docking procedure. The native ligand was first separated from the M^{pro}-ligand complex prior to redocking. The redocked ligand N3 was superimposed on the native ligand and RMSD was measured using Discovery Studio.

In silico drug-likeness and ADMET prediction

The drug-likeness properties of the compounds were assessed based on Lipinski's rule using Swis-

sADME (<http://www.swissadme.ch/index.php>). Molecular weight, hydrogen bond donor and acceptor, and logP of each compound were measured. The properties of absorption, distribution, metabolism, excretion and toxicity (ADMET) were predicted using SwissADME and admetSAR v2.0 (<http://lcmd.ecust.edu.cn/admetSAR2/>). The absorption of the compounds was evaluated based on the factors of gastrointestinal absorption and the status of either P-glycoprotein (P-gp) substrate or inhibitor. The ability of the compounds to cross the blood-brain barrier (BBB) was also predicted. The metabolism of the compounds was estimated based on CYP450-2D6 and CYP450-3A4. The probability of the compounds being toxic and carcinogenic was predicted based on AMES toxicity and carcinogenic status, respectively.

Data analysis

The interaction of the ligands and the protein receptors was characterized based on the binding energy estimated by Autodock Vina. The generated output file for each ligand consisted of the binding poses with their respective binding energies in kcal/mol. The ligands were ranked based on the binding energies, and the ligand showing the lowest binding energy was selected as the best docking conformation. The hydrogen and hydrophobic interactions of top-ranked compounds against the proteins were visualized to understand the inhibitory mechanism of the compounds. The physicochemical properties of the compounds were measured to determine the suitability of the compounds to be active oral drugs. The compounds with molecular weight <500 g/mol, hydrogen bond acceptors <10, hydrogen bond donors <5 and logP value <5 were considered suitable for use as active oral drugs as they did not violate Lipinski's rule. The pharmacokinetic properties of the compounds were also measured to predict the druggability of the compounds further. The absorption, distribution, metabolism, excretion, and toxicity of the compounds in the human body were assessed based on Cheng et al. (2012) and Daina and Zoete (2016). Compounds with a favorable ADMET profile were candidates for drug development.

RESULTS

Docking of *P. tenellus* and *K. parviflora* compounds against SARS-CoV-2 M^{pro}

The negative binding energies of *P. tenellus* and *K. parviflora* compounds against the protein receptors indicated the energy released following the interaction between the compounds and the receptors (Tables 1 and 2). Lower binding energy correlates with stronger binding conformation. Out of all the com-

pounds tested, eight top-ranked compounds docked against M^{PRO} were from *P. tenellus*, showing lower binding energies than the other compounds indicating that *P. tenellus* contains more potent compounds than *K. parviflora*. Of these, rutin exhibited the lowest binding energy of -9 kcal/mol, indicating it as the best-docked compound (Table 1). This was followed by ellagic acid glucoside, which was also from *P. tenellus* with a binding energy of -8.5 kcal/mol. Rutin formed three hydrogen bonds with residues located at the substrate binding region, Gly143, Glu166, and Asp187 (Fig. 1). This compound also interacted with residue Phe140, which was involved in the dimerization of M^{PRO}. Ellagic acid glucoside formed a hydrogen bond with one of the catalytic dyad residues, Cys145. In addition, this compound was bound to the substrate binding residues, Ser144, His163, Thr190, and Gln192 through hydrogen bonds and Met165 and Gln189 through hydrophobic interactions. Interestingly, rutin and ellagic acid glucoside showed higher binding conformations with M^{PRO} than the drugs nelfinavir, and hydroxychloroquine (Table 3). The higher binding efficiencies between these compounds and M^{PRO} were probably contributed by the higher number of hydrogen bonds formed in the com-

pounds-M^{PRO} complex compared to the drugs-M^{PRO} complex. Other than these compounds, ellagitannin and myricetin-rhamnoside also docked stronger with M^{PRO} than the drugs.

As for *K. parviflora*, 4-hydroxy-6-methoxyflavone showed the best binding conformation, with M^{PRO} exhibiting the lowest binding energy of -7.6 kcal/mol among the other compounds (Table 2). This compound formed strong hydrogen bonds with Glu166 and Asp187 of M^{PRO} and hydrophobic interaction with Met49, which were the residues responsible for substrate binding (Fig. 1). Besides, compound 5-hydroxy-3,7,4'-trimethoxyflavone also established a stronger binding conformation with M^{PRO} compared to the other compounds by interacting with the catalytic residue, Cys145 and the substrate binding residue, Ser144 through a hydrogen bond formation. The residues Thr26 and Leu141, which were adjacent to M^{PRO} dimerization site, also interacted with this compound. Even though both 4-hydroxy-6-methoxyflavone and 5-hydroxy-3,7,4'-trimethoxyflavone were not as potent as nelfinavir, they bound to M^{PRO} stronger than hydroxychloroquine (Table 3).

Table 1. Binding energy of *P. tenellus* compounds against M^{PRO} (PDB ID: 6LU7) and RdRp (PDB ID: 6M71).

No.	Compound names	Binding energy (kcal/mol)	
		6LU7	6M71
1	Rutin	-9.0	-9.0
2	Ellagic acid glucoside	-8.5	-8.2
3	Ellagitannin	-8.3	-10.5
4	Myricetin-rhamnoside	-8.3	-8.5
5	Chlorogenic acid derivatives	-8.0	-7.1
6	Quercetin glucoside	-7.8	-7.6
7	Dehydrohexahydroxy diphenic acid	-7.7	-7.8
8	Caffeic acid 3-glucoside	-7.7	-6.6
9	o-Coumaroylquinic acid	-7.6	-6.7
10	Coumaric acid	-7.4	-6.5
11	Caffeoylmalic acid	-7.3	-6.5
12	Catechin	-7.3	-6.8
13	2-O-caffeoyl glucarate	-7.2	-7.1
14	β-glucogallin	-7.1	-7.2
15	Brevifolin carboxylic acid	-6.9	-7.2
16	2,4-Dihydroxy-6-(3-methylbutoxy)-3-(3-methylbutyl) benzaldehyde	-5.8	-5.4
17	Gallic acid	-5.5	-5.9
18	Quinic acid	-5.4	-5.5
19	Brevifolin	-5.1	-5.0

Table 2. Binding energy of *K. parviflora* compounds against M^{pro} (PDB ID: 6LU7) and RdRp (PDB ID: 6M71).

No.	Compound names	Binding energy (kcal/mol)	
		6LU7	6M71
1	4-Hydroxy-6-methoxyflavone	-7.6	-6.4
2	5-Hydroxy-3,7,4'-trimethoxyflavone	-7.1	-6.5
3	4',5-Dihydroxy-7-methoxyflavone	-7.1	-6.6
4	5-Hydroxy-7-methoxyflavone	-7.1	-6.5
5	Peonidin	-7.0	-7.0
6	3-Methyl-5,7,4'-trimethoxyflavone	-7.0	-6.4
7	3-Methyl-5,7,3',4'-tetramethoxyflavone	-7.0	-6.3
8	5-Hydroxy-7,4'-dimethoxyflavone	-7.0	-6.6
9	3,5,7-Trimethoxyflavone	-6.9	-6.1
10	3,5,7-Trihydroxy-2-(4-hydroxy-3,5-dimethoxyphenyl)-chromenium	-6.9	-6.7
11	5-Hydroxy-7,3',4'-trimethoxyflavone	-6.9	-6.7
12	5-Hydroxy-3,7,3',4'-tetramethoxyflavone	-6.9	-6.6
13	Methoxyflavones	-6.9	-6.2
14	5,7-Dimethoxyflavone	-6.9	-6.3
15	3,5,7,3',4'-Pentamethoxyflavone	-6.8	-6.6
16	5,3'-Dihydroxy-3,7,4'-trimethoxyflavone	-6.8	-6.8
17	5-Hydroxy-3,7-dimethoxyflavone	-6.8	-6.4
18	3,5,7,4'-Tetramethoxyflavone	-6.8	-6.5
19	5,7,3',4'-Tetramethoxyflavone	-6.8	-6.5
20	5,7,4'-Trimethoxyflavone	-6.8	-6.4

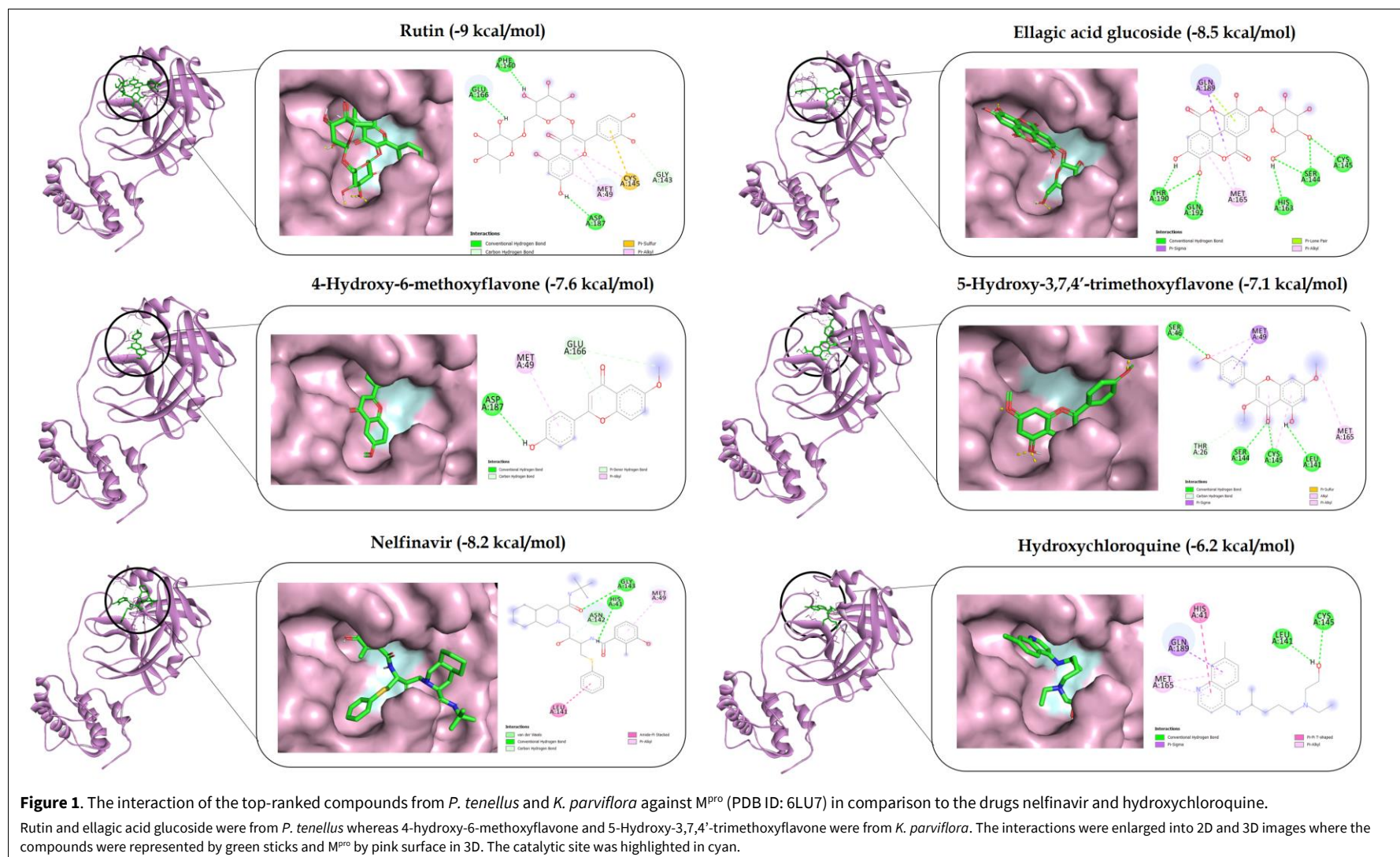
Table 3. Binding energy of the repurposing drugs (nelfinavir, remdesivir and hydroxychloroquine) and natural substrates (GTP, ATP, UTP and CTP) against M^{pro} (PDB ID: 6LU7) and RdRp (PDB ID: 6M71).

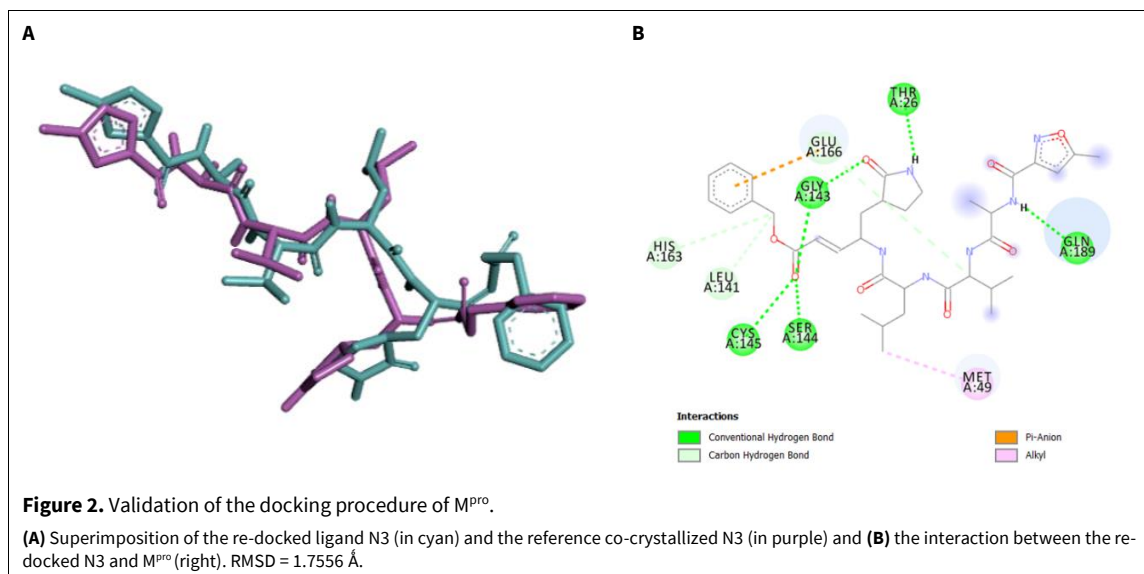
No.	Drug names	Binding energy (kcal/mol)	
		6LU7	6M71
1	Nelfinavir	-8.2	-
2	Remdesivir	-	-7.3
3	Hydroxychloroquine	-6.2	-5.4
4	GTP	-	-7.6
5	ATP	-	-7.6
6	UTP	-	-7.3
7	CTP	-	-7.1

To validate the docking procedure for M^{pro}, the re-docked ligand N3 was superimposed onto the reference co-crystallized N3. The re-docked N3 interacted with the residues Thr26, Met49, Leu141, Gly143, Ser144, Cys145, His163, Glu166, and Gln189 of M^{pro}, which were similar to those observed by Gentile et al. (2020) and Shivanika et al. (2020) (Fig. 2). An RMSD of 1.7556 Å was observed suggesting that the docking procedure was valid.

Docking of *P. tenellus* and *K. parviflora* compounds against SARS-CoV-2 RdRp

P. tenellus compounds showed inhibition potential against RdRp where ten of its compounds demonstrated the lowest binding energies among all the tested compounds, including *K. parviflora* compounds (Table 1). This indicated that *P. tenellus* has more effective compounds against RdRp than *K. parviflora*,





which was similar to the M^{pro} case. Out of these compounds, ellagitannin was the best docked-compound with a binding energy of -10.5 kcal/mol. Ellagitannin bound to one of the RdRp core catalytic residues, Asp761 and residues in the binding pocket of RdRp, Trp800, Glu811 and Ser814 through hydrogen bonds (Fig. 3). Hydrogen bonds were also formed with residues from the NTP entry channel, Arg553 and Arg555. Additional hydrogen bonds formed with residues His439, Ile548, Asp623 and Ser682 strengthened the interaction between ellagitannin and RdRp. Furthermore, a hydrophobic interaction was also formed with residue Lys798 involved in stabilizing the core structure of RdRp domain. Other than ellagitannin, rutin also strongly interacted with the catalytic residues, Asp760 and Asp761 at a low binding energy of -9 kcal/mol. This compound bound to the binding pocket residues of RdRp, Tyr619, Ser814 and Ser759. Compared to remdesivir (-7.3 kcal/mol) and hydroxychloroquine (-5.4 kcal/mol), interestingly, both ellagitannin and rutin were able to bind stronger with RdRp than the drugs. In addition, ellagic acid glucoside, myricetin-rhamnoside, quercetin glucoside, and dehydrohexahydroxy diphenic acid were also more potent than the drugs. Remdesivir interacted with the catalytic residues of RdRp, Asp760 and Asp761, and the NTP-entry channel residues, Arg553 and Arg555, which were in line with those reported by Aftab et al. (2020), Gao et al. (2020) and Eweas et al. (2021). This is also an indicative that the docking procedure for RdRp used in this study was acceptable and valid. In comparison to the NTP (GTP, ATP, CTP, and UTP) substrates, these compounds exhibited greater binding conformations with RdRp than the substrates themselves.

Likewise, the compounds from *K. parviflora* showed inhibition activity on RdRp. The top lowest energy compounds, peonidin and 5,3'-dihydroxy-3,7,4'-trimethoxyflavone, exhibited a binding energy of -7 and -6.8 kcal/mol, respectively, which were comparable with UTP (-7.3 kcal/mol) and CTP (-7.1 kcal/mol) suggesting that these compounds could be competitive ligands to the nucleotides. The compound 5,3'-dihydroxy-3,7,4'-trimethoxyflavone could even block the nucleotides binding to RdRp by forming a hydrogen bond with the residue Arg553 located at the NTP-entry channel (Fig. 3). On the other hand, peonidin interacted with the catalytic residue, Asp762, and the binding pocket residues, Tyr619, Glu811, and Ala762 through hydrogen bonds. In comparison to remdesivir and hydroxychloroquine, these compounds were more potent than hydroxychloroquine but not as potent as remdesivir.

In silico drug-likeness prediction

The compounds from *P. tenellus* and *K. parviflora* were assessed for their suitability as an oral active drug. All the compounds from *K. parviflora* and 13 compounds from *P. tenellus* passed Lipinski's rule of five, where these compounds have none or not more than one violation of the following criteria; molecular weight less than 500 g/mol, hydrogen bond acceptors less than 10, hydrogen bond donors less than 5 and logP value less than 5 (Table 4). The remaining six compounds from *P. tenellus* did not pass the Lipinski's rule by violating more than one of the criteria. This includes rutin, ellagic acid glucoside, and ellagitannin, which were the top compounds against M^{pro} and RdRp (Table 4).

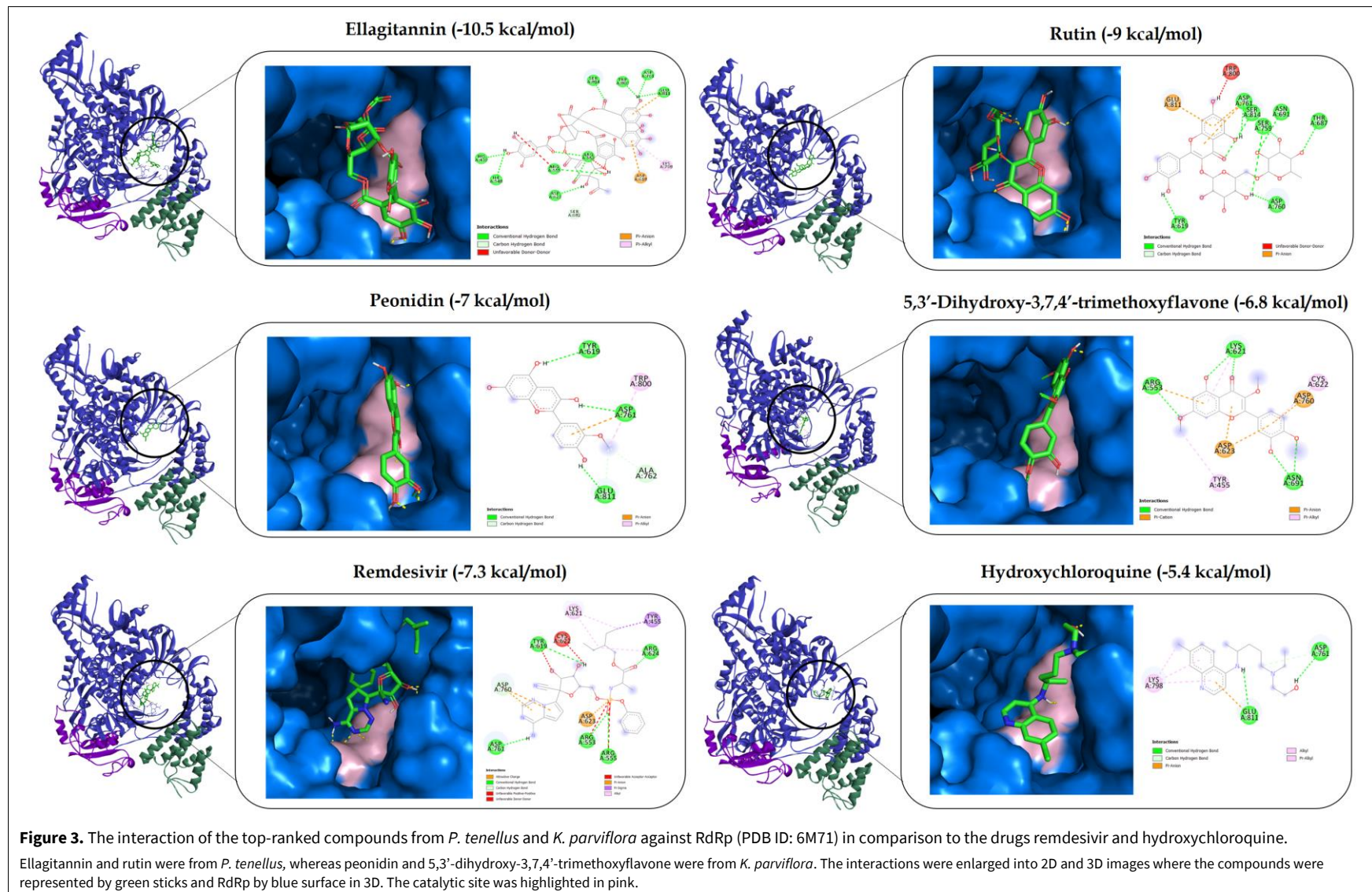


Table 4. Predicted drug-likeness and ADMET properties of the compounds from *P. tenellus* and *K. parviflora*.

Compound name	Drug-likeness					Absorption				Distri- bution	Metabolism					Toxicity	
	MW	H-bond acceptors	H-bond donors	LOGP	Lipinski violation	GI	Pgp substrate	Pgp inhibitor	BBB	Inhibitor					AMES toxicity	Carcino- genicity	
										CYP 1A2	CYP 2C19	CYP 2C9	CYP 2D6	CYP 3A4			
<i>P. tenellus</i>																	
Rutin*	610.52	16	10	-1.69	3	Low	Yes	No	No	No	No	No	No	No	No	No	
Ellagic acid glucoside*	464.33	13	7	-1.21	2	Low	No	No	No	No	No	No	No	No	Yes	No	
Ellagitannin*	992.71	27	13	-0.07	3	Low	Yes	No	No	No	No	No	No	No	No	No	
Quinic acid	192.17	6	5	-2.32	0	Low	No	No	No	No	No	No	No	No	No	No	
Caffeoylmalic acid	296.23	8	4	0.47	0	High	No	No	No	No	No	No	No	No	No	No	
Caffeic acid 3-glucoside	342.3	9	6	-1.44	1	Low	No	No	No	No	No	No	No	No	No	No	
o-coumaroylquinic acid	338.31	8	5	-0.46	0	Low	No	No	No	No	No	No	No	No	No	No	
Coumaric acid	326.3	8	5	-1.15	0	Low	No	No	No	No	No	No	No	No	Yes	No	
β-glucogallin	332.26	10	7	-2.24	1	Low	No	No	No	No	No	No	No	No	No	No	
2-O-caffeoyl glucarate	370.27	11	5	-4.5	1	Low	No	No	No	No	No	No	No	No	No	No	
2,4-Dihydroxy-6-(3-methylbutoxy)-3-(3-methyl-butyl) benzaldehyde	294.39	4	2	3.92	0	High	No	No	Yes	Yes	No	No	Yes	No	No	No	
Chlorogenic acid derivatives	354.31	9	6	-0.75	1	Low	No	No	No	No	No	No	No	No	No	No	
Quercetin glucoside	550.42	15	8	-0.51	3	Low	Yes	No	No	No	No	No	No	No	No	No	
Myricetin-rhamnoside	464.38	12	8	0.19	2	Low	No	No	No	No	No	No	No	No	No	No	
Catechin	290.27	6	5	1.22	0	High	Yes	No	No	No	No	No	No	No	No	No	
Gallic acid	170.12	5	4	0.5	0	High	No	No	No	No	No	No	No	Yes	No	No	
Brevifolin	196.2	4	1	1.61	0	High	No	No	Yes	No	No	No	No	No	No	No	
Brevifolin carboxylic acid	292.2	8	4	0.66	0	Low	No	No	No	No	No	No	No	No	Yes	No	
Dehydrohexahydroxy diphenic acid	354.22	11	7	-1.76	2	Low	No	No	No	No	No	No	No	No	No	No	

Table 4. Predicted drug-likeness and ADMET properties of the compounds from *P. tenellus* and *K. parviflora* (continued...)

Compound name	Drug-likeness					Absorption				Distri- bution	Metabolism					Toxicity	
	MW	H-bond acceptors	H-bond donors	LOGP	Lipinski violation	GI	Pgp substrate	Pgp inhibitor	BBB	Inhibitor					AMES toxicity	Carcino- genicity	
										CYP 1A2	CYP 2C19	CYP 2C9	CYP 2D6	CYP 3A4			
<i>K. parviflora</i>																	
4-Hydroxy-6-Methoxyflavone*	268.26	4	1	3.17	0	High	No	No	Yes	Yes	Yes	Yes	No	Yes	Yes	Yes	No
5-Hydroxy-3,7,4'-trimethoxyflavone*	328.32	6	1	3.19	0	High	No	Yes	Yes	Yes	No	Yes	Yes	Yes	No	No	No
Peonidin*	301.27	6	4	3.21	0	High	Yes	No	No	Yes	No	No	No	No	No	No	No
5,3'-dihydroxy-3,7,4'-trimethoxyflavone*	344.32	7	2	2.9	0	High	No	Yes	No	Yes	No	Yes	Yes	Yes	No	No	No
5-Hydroxy-3,7-dimethoxyflavone	298.29	5	1	3.18	0	High	No	Yes	Yes	Yes	Yes	Yes	Yes	Yes	No	No	No
5-Hydroxy-7-methoxyflavone	268.26	4	1	3.17	0	High	No	No	Yes	Yes	Yes	Yes	Yes	Yes	Yes	Yes	No
5-Hydroxy-7,4'-dimethoxyflavone	298.29	5	1	3.18	0	High	No	No	Yes	Yes	Yes	Yes	Yes	Yes	No	No	No
5-Hydroxy-3,7,3',4'-tetramethoxyflavone	358.34	7	1	3.2	0	High	No	Yes	No	Yes	No	Yes	Yes	Yes	No	No	No
5,7,3',4'-tetramethoxyflavone	342.34	6	0	3.49	0	High	No	Yes	Yes	Yes	Yes	Yes	Yes	Yes	No	No	No
3-Methyl-5,7,4'-trimethoxyflavone	326.34	5	0	3.79	0	High	No	Yes	Yes	Yes	Yes	Yes	No	Yes	No	No	No
3-Methyl-5,7,3',4'-tetramethoxyflavone	356.37	6	0	3.8	0	High	No	Yes	Yes	Yes	Yes	Yes	No	Yes	No	No	No
5-hydroxy-7,3',4'-trimethoxyflavone	328.32	6	1	3.19	0	High	No	Yes	Yes	Yes	Yes	Yes	Yes	Yes	No	No	No
4,4'-dihydroxy-6-methoxyflavone	284.26	5	2	2.88	0	High	No	No	No	Yes	No	Yes	Yes	Yes	Yes	Yes	No
3,5,7-trihydroxy-2-(4-hydroxy-3,5-dimethoxy-phenyl)chromenium	331.3	7	4	3.22	0	High	Yes	No	No	Yes	No	No	No	No	No	No	No
3,5,7,4'-tetramethoxyflavone	342.34	6	0	3.49	0	High	No	No	Yes	Yes	Yes	Yes	Yes	Yes	No	No	No
Methoxyflavones	252.26	3	0	3.47	0	High	No	Yes	Yes	Yes	Yes	Yes	Yes	Yes	No	No	No
3,5,7-trimethoxyflavone	312.32	5	0	3.49	0	High	No	Yes	Yes	Yes	Yes	Yes	Yes	Yes	No	No	No
5,7-dimethoxyflavone	282.29	4	0	3.48	0	High	No	Yes	Yes	Yes	Yes	Yes	Yes	Yes	No	No	No
3,5,7,3',4'-pentamethoxyflavone	372.37	7	0	3.5	0	High	No	Yes	Yes	No	Yes	Yes	No	Yes	Yes	Yes	No
5,7,4'-trimethoxyflavone	312.32	5	0	3.49	0	High	No	Yes	Yes	Yes	Yes	Yes	Yes	Yes	No	No	No

* Top compounds against Mpro and RdRp

Rutin, ellagic acid glucoside, and ellagitannin were predicted to be poorly absorbed by the human gastrointestinal tract upon oral administration. Rutin and ellagitannin were substrates and non-inhibitors of P-gp, indicating that these compounds could be effluxed from the cells. Instead, ellagic acid glucoside was a non-substrate of P-gp. Moreover, these three compounds were unable to cross the BBB but were non-inhibitors of CYP450 enzymes, CYP2D6 and CYP3A4, which are indispensable for drug metabolism in the liver. These compounds were also predicted to be non-carcinogens and non-toxic except for ellagic acid glucoside, which was possibly toxic.

In contrast, the top compounds from *K. parviflora*, 4-hydroxy-6-methoxyflavone, 5-hydroxy-3,7,4'-trimethoxyflavone, peonidin and 5,3'-dihydroxy-3,7,4'-trimethoxyflavone have high potentials to be oral active drugs as these compounds obey all of Lipinski's rule criteria (Table 4). These compounds could be efficiently absorbed in the gastrointestinal tract. They were also P-gp non-substrates except for peonidin. The compounds 5-hydroxy-3,7,4'-trimethoxyflavone and 5,3'-dihydroxy-3,7,4'-trimethoxyflavone were even P-gp inhibitors suggesting that they could prevent drug efflux and have better absorption (Amin, 2013). Furthermore, 4-hydroxy-6-methoxyflavone and 5-hydroxy-3,7,4'-trimethoxyflavone could permeate through the BBB. However, 4-hydroxy-6-methoxyflavone, 5-hydroxy-3,7,4'-trimethoxyflavone, and 5,3'-dihydroxy-3,7,4'-trimethoxyflavone could have poor metabolism by being inhibitors of CYP2D6 and CYP3A4. Only peonidin was predicted to be CYP2D6 and CYP3A4 non-inhibitors, indicating that this compound was possibly able to be metabolized in the liver. In terms of toxicity, all of these compounds were non-carcinogens, and they were also non-toxic except for 4-hydroxy-6-methoxyflavone.

DISCUSSION

P. tenellus and *K. parviflora* are medicinal herbs composed of valuable bioactive compounds with multiple biological activities. Hydrosable tannins such as ellagitannin, ellagic acid glucoside, and dehydrohexahydroxy diphenic acid are the most abundant compounds found in *P. tenellus* which have been proven to possess antiviral activity (Mohd Jusoh et al., 2019; Nutan et al., 2013; Tan et al., 2013). In addition, *P. tenellus* is rich in flavonoids such as rutin, myricetin-rhamnoside, and quercetin glucoside, which are commonly associated with antiviral properties against HIV, influenza and other viruses (Mehrbood et al., 2021; Ortega et al., 2017; Tao et al., 2007). Likewise, *K. parviflora* also contains flavonoids abundantly.

Methoxyflavone and its derivatives found in this herb have been shown to efficiently inhibit HIV-1, HCV, and HCMV proteases (Sookkongwaree et al., 2006). Since then, *P. tenellus* and *K. parviflora* have become interesting sources of natural antivirals.

In this study, the ability of the compounds from *P. tenellus* and *K. parviflora* to inhibit two major targets of SARS-CoV-2, M^{Pro} and RdRp, was proven through *in silico* studies. M^{Pro} and RdRp are two vital SARS-CoV-2 proteins involved in viral polyprotein proteolysis and viral replication and transcription, respectively (Jin et al., 2021). M^{Pro} is a homodimer consisting of two protomers in which each protomer contains three domains (domains I, II and III). The catalytic dyad (His41 and Cys145) and the substrate binding sites are located in a cleft in between domains I and II. The substrate binding site, comprising the residues His41, Met49, Gly143, Ser144, His163, His164, Met165, Glu166, Leu167, Asp187, Arg188, Gln189, Thr190, Ala191 and Gln192, is highly conserved among M^{Pro}s from other coronaviruses as well as SARS-CoV-2 variants (Pitts et al., 2022). Thus, the inhibitors targeting this site should have a broad-spectrum antiviral activity. It is interesting that rutin and ellagic acid glucoside from *P. tenellus*, as well as 4-hydroxy-6-methoxyflavone and 5-hydroxy-3,7,4'-trimethoxyflavone from *K. parviflora* were able to efficiently bind to the substrate binding site that was not only predicted to block the catalytic activity of M^{Pro} but also could be effective against all the emergent SARS-CoV-2 variants. However, additional *in silico* studies and further physical experiments should be conducted to verify this.

In addition, rutin bound to the residue Phe140, which was a part of the dimer interface located in the domain III of M^{Pro}. The dimerization process is crucial for the formation of the homodimer, which is an active form of M^{Pro} and is necessary for enzyme activity as it assists in the formation of the correct orientation of the substrate binding site (Goyal and Goyal, 2020). A salt bridge interaction between Glu290 of one protomer and Arg4 of another protomer occurs in this process (Zhang et al., 2020). The ability of rutin to bind to both the dimerization and the substrate binding sites suggested that this compound could disrupt the formation of an active structure of M^{Pro} thus blocking the M^{Pro} catalytic activity.

The polyprotein proteolysis activity mediated by SARS-CoV-2 M^{Pro} produces multiple nsps, which perform numerous functions in the viral replication and assembly processes (Xue et al., 2014). In the nsps complex, nsp12, which is also called as RdRp, is the core component responsible for the elongation of a new RNA chain from an RNA template (te Velthuis et

al., 2010). The catalytic activity of RdRp is assisted by its partners, nsp7 and nsp8 where the partners aid in increasing the efficiency of RNA synthesis (te Velthuis et al., 2012). The RNA polymerization process mediated by RdRp includes template entry and binding, NTP entry and binding, and polymerization. Similar to M^{pro}, the catalytic domain of RdRp is also conserved among SARS-CoV-2 variants and other coronaviruses, suggesting that the inhibitors targeting RdRp might be broadly effective (Martin et al., 2021). Other than the catalytic site, RdRp activity is also assisted by the NTP-entry channel formed by the hydrophilic residues Lys545, Arg553, and Arg555 (Long et al., 2021). The NTP substrates enter and bind to the channel simultaneously as the RNA template enters the RdRp catalytic site leading to the initiation of the RNA polymerization process (Gao et al. 2020).

Remdesivir is a SARS-CoV-2 RdRp inhibitor where it is evidently effective in targeting RdRp by interacting with the catalytic and NTP-binding residues (Gao et al., 2020; Eweas et al., 2021). However, in this study, the compounds ellagitannin, rutin, ellagic acid glucoside, myricetin-rhamnoside, quercetin glucoside, and dehydrohexahydroxy diphenic acid from *P. tenellus* demonstrated greater binding conformations with RdRp than remdesivir by interacting with the catalytic residues that were anticipated to stop RNA polymerization. Interestingly, these compounds were also able to bind stronger to the NTP-entry channel than the NTPs (GTP, ATP, UTP, and CTP) themselves, indicating that these compounds could efficiently block the binding of NTPs to RdRp that subsequently arrests the SARS-CoV-2 RNA replication. Moreover, ellagitannin could also disrupt the stability of the RdRp core structure by interacting with the residue Lys798. Similarly, peonidin and 5,3'-dihydroxy-3,7,4'-trimethoxyflavone from *K. parviflora* were able to form a stable conformation with RdRp and might be competitive ligands to the NTPs. Although these compounds were not as potent as remdesivir and the top compounds from *P. tenellus*, they showed stronger inhibitory activity than hydroxychloroquine. Hence, it is proposed that the aforementioned compounds could be effective SARS-CoV-2 RdRp inhibitors.

Prior to the development of a drug, the drug-likeness and ADMET properties of the compounds were assessed to predict their ability to be qualified as drug candidates. The compounds from *K. parviflora*, particularly 4-hydroxy-6-methoxyflavone, 5-hydroxy-3,7,4'-trimethoxyflavone, peonidin and 5,3'-dihydroxy-3,7,4'-trimethoxyflavone, were predicted to be potential oral drugs besides having potent inhibition activity against SARS-CoV-2 M^{pro} and RdRp. However, in contrast, rutin, ellagic acid glucoside, and ellag-

itannin from *P. tenellus* were less potential to be oral drugs and exhibited poor ADMET properties, although they exerted strong inhibitory activities against M^{pro} and RdRp. The large molecular weight and high number of aromatic rings of these compounds possibly affect the compound absorption and permeability, which consequently reduces the drug-likeness potential of the compounds (Ritchie and Macdonald, 2009). However, structural modification and nanotechnology employment may aid in improving the ADMET properties of these compounds as potent drugs (Farouk and Shamma, 2019).

CONCLUSION

P. tenellus compounds, particularly rutin and ellagic acid glucoside, as well as *K. parviflora* compounds, 4-hydroxy-6-methoxyflavone and 5-hydroxy-3,7,4'-trimethoxyflavone were proposed as effective inhibitors of SARS-CoV-2 M^{pro}. Rutin and ellagitannin from *P. tenellus* and peonidin and 5,3'-dihydroxy-3,7,4'-trimethoxyflavone from *K. parviflora* could be potent SARS-CoV-2 RdRp inhibitors. In terms of drug-likeness, the *K. parviflora* compounds were predicted to have a higher potential to be oral drugs than the *P. tenellus* compounds. Structural modification of *P. tenellus* compounds is required to improve their drug-likeness properties. In addition, *in vitro* and *in vivo* studies must be implemented to provide further evidence to support the findings of this study. Overall, this study provides potential candidates for the development of plant-based inhibitors of SARS-CoV-2 M^{pro} and RdRp.

CONFLICT OF INTEREST

The authors declare no conflicts of interest.

ACKNOWLEDGMENTS

The authors thank the Malaysian Agricultural Research and Development Institute (MARDI) for the Special Project (Grant No. SRB0333515) for funding this study.

REFERENCES

- Aftab SO, Ghouri MZ, Masood MU, Haider Z, Khan Z, Ahmad A, Munawar N (2020) Analysis of SARS-CoV-2 RNA-dependent RNA polymerase as a potential therapeutic drug target using a computational approach. *J Transl Med* 18(1): 275. <https://doi.org/10.1186/s12967-020-02439-0>
- Amin ML (2013) P-glycoprotein inhibition for optimal drug delivery. *Drug Target Insights* 7: 27-34. <https://doi.org/10.33393/dti.2013.1349>
- Babar M, Najam-U-Sahar SZ, Ashraf M, Kazi AG (2013) Antiviral drug therapy - Exploiting medicinal plants. *J Antivir Antiretrovir* 5: 28-36. <https://doi.org/10.4172/2155-6113.1000215>
- Ben-Shabat S, Yarmolinsky L, Porat D, Dahan A (2020) Antiviral effect of phytochemicals from medicinal plants: Applications

- and drug delivery strategies. *Drug Deliv Transl Res* 10(2): 354–367. <https://doi.org/10.1007/s13346-019-00691-6>
- Chen D, Li H, Li W, Feng S, Deng D (2018) *Kaempferia parviflora* and its methoxyflavones: Chemistry and biological activities. *Evid Based Complement Alternat Med* 2018: 4057456. <https://doi.org/10.1155/2018/4057456>
- Cheng F, Li W, Zhou Y, Shen J, Wu Z, Liu G, Lee PW, Tang Y (2012) admetSAR: a comprehensive source and free tool for assessment of chemical ADMET properties. *J Chem Inf Model* 52(11): 3099–3105. <https://doi.org/10.1021/ci300367a>
- Cheng PW, Ng LT, Chiang LC, Lin CC (2006) Antiviral effects of saikosaponins on human coronavirus 229E *in vitro*. *Clin Exp Pharmacol Physiol* 33(7): 612–616. <https://doi.org/10.1111/j.1440-1681.2006.04415.x>
- Daina A, Zoete V (2016) A BOILED-Egg to predict gastrointestinal absorption and brain penetration of small molecules. *ChemMedChem* 11: 1117–1121. <https://doi.org/10.1002/cmdc.201600182>
- Eweas AF, Alhossary AA, Abdel-Moneim AS (2021) Molecular docking reveals ivermectin and remdesivir as potential repurposed drugs against SARS-CoV-2. *Front Microbiol* 11: 592908. <https://doi.org/10.3389/fmicb.2020.592908>
- Farouk F, Shamma R (2019) Chemical structure modifications and nano-technology applications for improving ADME-Tox properties, a review. *Arch Pharm Chem Life Sci* 352(2): e1800213. <https://doi.org/10.1002/ardp.201800213>
- Jin Z, Wang H, Duan Y, Yang H (2020) The main protease and RNA-dependent RNA polymerase are two prime targets for SARS-CoV-2. *Biochem Biophys Res Commun* 538: 63–71. <https://doi.org/10.1016/j.bbrc.2020.10.091>
- Gao Y, Yan L, Huang Y, Liu F, Zhao Y, Cao L, Wang T, Sun Q, Ming Z, Zhang L, Ge J, Zheng L, Zhang Y, Wang H, Zhu Y, Zhu C, Hu T, Hua T, Zhang B, Yang X, Li J, Yang H, Liu Z, Xu W, Guddat LW, Wang Q, Lou Z, Rao Z (2020) Structure of the RNA-dependent RNA polymerase from COVID-19 virus. *Science* 368: 779–782. <https://doi.org/10.1126/science.abb7498>
- Gentile D, Patamia V, Scala A, Sciortino MT, Piperno A, Rescifina (2020) Putative inhibitors of SARS-CoV-2 main protease from a library of marine natural products: A virtual screening and molecular modeling study. *Mar Drugs* 18(4): 225. <https://doi.org/10.3390/md18040225>
- Ghanimi R, Ouhammou A, El Atki Y, Cherkaoui M (2022) Molecular docking study of the main phytochemicals of some medicinal plants used against COVID-19 by the rural population of Al-Haouz region, Morocco. *J Pharm Pharmacogn Res* 10(2): 227–238. https://doi.org/10.56499/jppres21.1200_10.2.227
- Goyal B, Goyal D (2020) Targeting the dimerization of the main protease of coronaviruses: A potential broad-spectrum therapeutic strategy. *ACS Comb Sci* 22(6): 297–305. <https://doi.org/10.1021/acscombsci.0c00058>
- Kharisma VD, Aghata A, Ansori ANM, Widyananda MH, Rizky WC, Dings TGA, Derkho M, Lykasova I, Antonius Y, Rosadi I, Zainul R (2022) Herbal combination from *Moringa oleifera* Lam. and *Curcuma longa* L. as SARS-CoV-2 antiviral via dual inhibitor pathway: A viroinformatics approach. *J Pharm Pharmacogn Res* 10(1): 138–146. https://doi.org/10.56499/jppres21.1174_10.1.138
- Lamb YN (2022) Nirmatrelvir plus ritonavir: first approval. *Drugs* 82: 585–591. <https://doi.org/10.1007/s40265-022-01692-5>
- Long C, Romero ME, La Rocco D, Yu J (2021) Dissecting nucleotide selectivity in viral RNA polymerases. *Comput Struct Biotechnol J* 19: 3339–3348. <https://doi.org/10.1016/j.csbj.2021.06.005>
- Martin R, Li J, Parvangada A, Perry J, Cihlar T, Mo H, Porter D, Svarovskaia E (2021) Genetic conservation of SARS-CoV-2 RNA replication complex in globally circulating isolates and recently emerged variants from humans and minks suggests minimal pre-existing resistance to remdesivir. *Antiviral Res* 188: 105033. <https://doi.org/10.1016/j.antiviral.2021.105033>
- Mehrbod P, Hudy D, Shyntum D, Markowski J, Łos MJ, Ghavami S (2021) Quercetin as a natural therapeutic candidate for the treatment of influenza virus. *Biomol* 11(1): 10. <https://doi.org/10.3390/biom11010010>
- Mohammad Zadeh N, Mashinchi Asl NS, Forouharnejad K, Ghadimi K, Parsa S, Mohammadi S, Omidi A (2021) Mechanism and adverse effects of COVID-19 drugs: a basic review. *Int J Physiol Pathophysiol Pharmacol* 13(4): 102–109.
- Mohd Jusoh NH, Subki A, Yeap SK, Yap KC, Jaganath IB (2019) Pressurized hot water extraction of hydrosable tannins from *Phyllanthus tenellus* Roxb. *BMC Chem* 13(1): 134. <https://doi.org/10.1186/s13065-019-0653-0>
- Nutan MM, Goel T, Das T, Malik S, Suri S, Rawat AKS, Srivastava SK, Tuli R, Malhotra S, Gupta SK (2013) Ellagic acid & gallic acid from *Lagerstroemia speciosa* L. inhibit HIV-1 infection through inhibition of HIV-1 protease & reverse transcriptase activity. *Indian J Med Res* 137: 540–548.
- Oh C, Price J, Brindley MA, Widrechner MP, Qu L, McCoy JA, Murphy P, Hauck C, Maury W (2011) Inhibition of HIV-1 infection by aqueous extracts of *Prunella vulgaris* L. *Virology* 438: 188. <https://doi.org/10.1016/j.virol.2011.07.018>
- Ortega JT, Suárez AI, Serrano ML, Baptista J, Pujol FH, Rangel HR (2017) The role of the glycosyl moiety of myricetin derivatives in anti-HIV-1 activity *in vitro*. *AIDS Res Ther* 14(1): 57. <https://doi.org/10.1186/s12981-017-0183-6>
- Pitts J, Li J, Perry JK, Du Pont V, Riola N, Rodriguez L, Lu X, Kurhade C, Xie X, Camus G, Manhas S, Martin R, Shi PY, Cihlar T, Porter DP, Mo H, Maiorova E, Bilello JP (2022) Remdesivir and GS-441524 retain antiviral activity against delta, omicron, and other emergent SARS-CoV-2 variants. *Antimicrob Agents Chemother* 66(6): e0022222. <https://doi.org/10.1128/aac.00222-22>
- Ritchie TJ, Macdonald SJ (2009) The impact of aromatic ring count on compound developability—are too many aromatic rings a liability in drug design? *Drug Discovery Today* 14(21/22): 1011–1020. <https://doi.org/10.1016/j.drudis.2009.07.014>
- Shivanika C, Deepak Kumar S, Venkataraghavan R, Pawan T, Sumitha A, Brindha Devi P (2020) Molecular docking, validation, dynamics simulations, and pharmacokinetic prediction of natural compounds against the SARS-CoV-2 main-protease. *J Biomol Struct Dyn* 40(2): 585–611. <https://doi.org/10.1080/07391102.2020.1815584>
- Silva T, Veras Filho J, Lúcia CDAE, Antonia DSI, Albuquerque U, Cavalcante de Araújo E (2012) Acute toxicity study of stone-breaker (*Phyllanthus tenellus* Roxb.). *Rev Cienc Farm* 33: 205–210.
- Sookkongwaree K, Geitmann M, Roengsumran S, Petsom A, Danielson UH (2006) Inhibition of viral proteases by Zingiberaceae extracts and flavones isolated from *Kaempferia parviflora*. *Pharmazie* 61(8): 717–721.
- Sornpet B, Potha T, Tragoolpua Y, Pringproa K (2017) Antiviral activity of five Asian medicinal plant crude extracts against highly pathogenic H5N1 avian influenza virus. *Asian Pac J Trop Med* 10(9): 871–876. <https://doi.org/10.1016/j.apjtm.2017.08.010>
- Tai W, He L, Zhang X, Pu J, Voronin D, Jiang S, Zhou Y, Du L (2020) Characterization of the receptor-binding domain (RBD) of 2019 novel coronavirus: Implication for development of RBD protein as a viral attachment inhibitor and vaccine. *Cell*

- Mol Immunol 17(6): 613–620. <https://doi.org/10.1038/s41423-020-0400-4>
- Tan WC, Jaganath IB, Manikam R, Sekaran SD (2013) Evaluation of antiviral activities of four local Malaysian *Phyllanthus* species against herpes simplex viruses and possible antiviral target. *Int J Med Sci* 10(13): 1817–1829. <https://doi.org/10.7150/ijms.6902>
- Tao J, Hu Q, Yang J, Li R, Li X, Lu C, Chen C, Wang L, Shattock R, Ben K (2007) *In vitro* anti-HIV and -HSV activity and safety of sodium rutin sulfate as a microbicide candidate. *Antiviral Res* 75(3): 227–233. <https://doi.org/10.1016/j.antiviral.2007.03.008>
- te Velthuis AJ, Arnold JJ, Cameron CE, van den Worm SH, Snijder EJ (2010) The RNA polymerase activity of SARS-coronavirus nsp12 is primer dependent. *Nucleic Acids Res* 38(1): 203–214. <https://doi.org/10.1093/nar/gkp904>
- te Velthuis AJ, van den Worm SH, Snijder EJ (2012) The SARS-coronavirus nsp7+nsp8 complex is a unique multimeric RNA polymerase capable of both de novo initiation and primer extension. *Nucleic Acids Res* 40(4): 1737–1747. <https://doi.org/10.1093/nar/gkr893>
- Vangeel L, Chiu W, De Jonghe S, Maes P, Slechten B, Raymenants J, André E, Leyssen P, Neyts J, Jochmans D (2022) Remdesivir, Molnupiravir and Nirmatrelvir remain active against SARS-CoV-2 Omicron and other variants of concern. *Antiviral Res* 198: 105252. <https://doi.org/10.1016/j.antiviral.2022.105252>
- Xue B, Blocquel D, Habchi J, Uversky AV, Kurgan L, Uversky VN, Longhi S (2014) Structural disorder in viral proteins. *Chem Rev* 114(13): 6880–6911. <https://doi.org/10.1021/cr400569z>
- Yenjai C, Prasanphen K, Daodee S, Wongpanich V, Kittakoop P (2004) Bioactive flavonoids from *Kaempferia parviflora*. *Fitoterapia* 75(1): 89–92. <https://doi.org/10.1016/j.fitote.2003.08.017>
- Zhang L, Lin D, Sun X, Curth U, Drosten C, Sauerhering L, Becker S, Rox K, Hilgenfeld R (2020) Crystal structure of SARS-CoV-2 main protease provides a basis for design of improved a-ketoamide inhibitors. *Science* 368: 409–412. <https://doi.org/10.1126/science.abb3405>
- Zhou P, Yang XL, Wang XG, Hu B, Zhang L, Zhang W, Si HR, Zhu Y, Li B, Huang CL, Chen HD, Chen J, Luo Y, Guo H, Jiang RD, Liu MQ, Chen Y, Shen XR, Wang X, Zheng XS, Zhao K, Chen QJ, Deng F, Liu LL, Yan B, Zhan FX, Wang YY, Xiao GF, Shi ZL (2020) Addendum: A pneumonia outbreak associated with a new coronavirus of probable bat origin. *Nature* 588(7836): E6. <https://doi.org/10.1038/s41586-020-2951-z>
- Zhu Z, Lian X, Su X, Wu W, Marraro GA, Zeng Y (2020) From SARS and MERS to COVID-19: A brief summary and comparison of severe acute respiratory infections caused by three highly pathogenic human coronaviruses. *Respir Res* 21(1): 224. <https://doi.org/10.1186/s12931-020-01479-w>

AUTHOR CONTRIBUTION:

Contribution	Supian S	Ahmad MA	Rozano L	Chandradevan M	Ab Rahman Z
Concepts or ideas	x		x	x	x
Design	x				
Definition of intellectual content	x		x	x	x
Literature search	x				
Experimental studies	x	x			
Data acquisition	x	x			
Data analysis	x	x			
Statistical analysis	x	x			
Manuscript preparation	x				
Manuscript editing	x	x	x		
Manuscript review	x	x	x	x	x

Citation Format: Supian S, Ahmad MA, Rozano L, Chandradevan M, Ab Rahman Z (2022) *Phyllanthus tenellus* Roxb. and *Kaempferia parviflora* Wall. ex Baker compounds as inhibitors of SARS-CoV-2 main protease and RNA-dependent RNA polymerase: A molecular docking study. *J Pharm Pharmacogn Res* 10(6): 1103–1116. https://doi.org/10.56499/jppres22.1485_10.6.1103

Publisher's Note: All claims expressed in this article are solely those of the authors and do not necessarily represent those of their affiliated organizations, or those of the publisher, the editors and the reviewers. Any product that may be evaluated in this article, or claim that may be made by its manufacturer, is not guaranteed or endorsed by the publisher.

Open Access: This article is distributed under the terms of the Creative Commons Attribution 4.0 International License (<http://creativecommons.org/licenses/by/4.0/>), which permits use, duplication, adaptation, distribution and reproduction in any medium or format, as long as you give appropriate credit to the original author(s) and the source, provide a link to the Creative Commons license and indicate if changes were made.